Progress in Fractional Differentiation and Applications
An International Journal

http://dx.doi.org/10.18576/pfda/120207

Assessment of Brucellosis Dynamics Through Fractional-Order Models with Empirical Validation

Sanjay Bhatter [1], *Sangeeta Kumawat* [1], *Sunil Dutt Purohit*[2], *Ali Akgül* [3,4,*], *and Mohamed Hafez*[5,6]

[1] Department of Mathematics, Malaviya National Institute of Technology Jaipur, India
[2] Department of HEAS (Mathematics), Rajasthan Technical University, Kota, India
[3] Department of Electrical and Electronics Engineering, Faculty of Engineering, Karadeniz Technical University, Trabzon, Turkey
[4] Department of Mathematics, Art and Science Faculty, Siirt University, 56100 Siirt, Turkey
[5] Faculty of Engineering and Quantity Surveying INTI, IU, Universi, Nilai, Malaysia
[6] Faculty of Management, Shinawatra University, Pathum Thani, Thailand

Received: 15 Jan. 2026, Revised: 18 Feb. 2026, Accepted: 2 Mar. 2026
Published online: 1 Apr. 2026

Abstract: The study represents a comprehensive fractional-order modeling framework for the transmission dynamics of brucellosis, incorporating Caputo–Fabrizio (CF) and Atangana–Baleanu in Caputo (ABC) sense operators. The primary objective is to investigate how different fractional operators and derivative orders influence the temporal progression and long-term persistence of brucellosis. To achieve this, we estimate the model parameters using the least-squares method, calibrated against real epidemiological data from mainland China. We also provide a qualitative analysis establishing the existence and uniqueness of solutions under the CF and ABC formulations. For numerical simulations, we implement the Adams–Bashforth predictor–corrector method and employ it across a range of fractional orders to visualize the evolution of all model compartments. Through comparative analysis, we find that fractional models capture memory effects more effectively than the classical approach, with the ABC operator yielding the closest fit to observed data. These findings underscore the effectiveness of fractional operators in modeling the chronic and persistent behavior of brucellosis.

Keywords: Brucellosis, cf fractional operator, abc fractional operator, parameter estimation, numerical simulations. good health and well-being, zero hungeri industry, innovation and infrastructure, life on land, zoonotic disease surveillance and control, one health–based mathematical modeling.

1 Introduction

Zoonotic diseases, which can be transmitted from animals to humans either directly through contact or indirectly via contaminated food, water, or environmental exposure, represent a persistent global health concern. Among them, brucellosis, caused by bacteria of the genus Brucella, remains one of the most widespread and under-recognized zoonoses, affecting both human and animal populations [1]. Each year, approximately 500,000 new cases are reported across more than 160 countries, with the highest burden observed in regions such as Central Asia, the Middle East, China, and parts of North and East Africa. The disease affects a wide range of livestock species and is primarily transmitted through contact with infected animals, reproductive discharges, or the consumption of unpasteurized dairy products. One of the most concerning aspects of brucellosis is the environmental resilience of the pathogen. Brucella organisms can survive for extended periods outside the host, particularly under cool and moist conditions, facilitating indirect transmission and making eradication particularly challenging [2]. From an agricultural perspective, the disease affects the economic growth due to reproductive failures such as abortion, stillbirth, infertility, prolonged calving intervals, and decreased milk yield. Human brucellosis, meanwhile, is mainly acquired through the consumption of unpasteurized dairy products or through occupational exposure to infected animals. Individuals such as farmers, veterinarians, abattoir workers, and laboratory personnel are therefore at heightened risk [3]. The human disease can manifest as acute, subacute, or chronic forms and is often misdiagnosed due to its nonspecific clinical symptoms.

* Corresponding author e-mail: aakgul1@upvnet.upv.es

Chronic brucellosis, in particular, is difficult to treat, typically requiring prolonged antibiotic therapy, and continues to pose a public health challenge in endemic regions [4].

Mathematical modeling offers a powerful framework to study the transmission dynamics and control strategies of infectious diseases [5, 6]. A number of models have been proposed in recent years to understand its spread across animal and human populations, incorporating direct and indirect transmission, environmental contamination, and vaccination interventions [7, 8]. More recently, fractional calculus has gained prominence in epidemiological modeling due to its ability to incorporate memory effects and hereditary properties of biological processes [9, 10]. Fractional-order differential equations [11–13] provide a natural framework to describe systems whose future evolution depends not only on the current state but also on past states. This non-local behavior is relevant in modeling infectious diseases with delayed or cumulative effects. Unlike classical integer-order models, fractional-order systems can capture the temporal evolution of infections more accurately, particularly in chronic diseases where past states influence current dynamics [14, 15]. Various definitions of fractional derivatives have been developed and applied to disease models, including the Caputo, CF, and ABC operators. Each characterized by distinct kernel functions and mathematical properties.The Caputo derivative, which features a singular power-law kernel, is widely used for its compatibility with standard initial conditions. In contrast, the CF derivative employs an exponential kernel, and the ABC operator is based on the Mittag-Leffler (ML) function, both of which introduce non-singular memory effects that are often more stable and computationally advantageous.

Several studies have demonstrated the effectiveness of fractional-order models in improving the descriptive and predictive accuracy of infectious disease models [16, 17]. Studies have shown that fractional-order epidemic models tend to yield improved data fitting, better long-term forecasts, and richer dynamical behavior compared to their integer-order counterparts [18–20]. This has led to a growing body of literature employing fractional models to study a wide range of diseases. Yapiskan et al. [21] investigated brucellosis dynamics across species using the Atangana–Baleanu (AB) fractional derivative, emphasizing the role of memory effects in interspecies transmission and demonstrating that fractional modeling better captures the long-term persistence of infection. In [22], a fractional brucellosis model was formulated using the CF operator, showing that the non-singular exponential kernel improved the representation of gradual infection buildup and environmental decay. The authors in [23, 30] introduced a model for bovine brucellosis in cattle by incorporating treatment and a saturation effect, utilizing a combination of fractal and fractional derivatives to account for nonlinear and memory-driven processes.

Despite the progress in this direction, most existing models focus on isolated operators or limited scenarios, making it difficult to compare how different fractional derivatives impact the overall disease dynamics. The present study seeks to address this gap by building upon the model developed by Hdaibat et al. [24], who formulated a brucellosis model using the Caputo fractional derivative and performed parameter estimation based on human case data from mainland China. Their work demonstrated that the fractional-order system provided a better fit than its integer-order counterpart, yet it remained limited to the Caputo formulation. Motivated by this limitation, our study extends the same model using two alternative non-singular fractional derivatives, the CF and ABC operators. Both of these operators possess advantageous mathematical properties, including finite memory kernels and improved numerical stability, which make them suitable for capturing the long-term, persistent behavior of chronic infections such as brucellosis. In this work, we estimate model parameters under each formulation using real epidemiological data and compare the dynamics of the disease across the Caputo, CF, and ABC operators, alongside the integer-order case. Through this comparative analysis, we aim to evaluate the influence of different memory kernels on disease transmission and assess which operator yields the most biologically consistent and data-accurate representation of brucellosis dynamics.

The structure of the remainder of the paper is as follows. Section 2 outlines the essential mathematical preliminaries related to fractional calculus, with a focus on the definitions of the CF and ABC derivatives. Section 3 presents the fractional-order brucellosis model reformulated under these two operators. In Section 4, we provide a qualitative analysis, including the existence and uniqueness of solutions, as well as the parameter estimation process for both models. Section 5 describes the numerical method used to solve the CF and ABC models. Section 6 presents the simulation results and graphical illustrations, offering a detailed examination of the dynamic behavior of the system under various fractional orders. Finally, Section 7 concludes the study by summarizing the key findings and discussing their implications.

2 Preliminaries

This section provides some preliminaries about fractional derivatives and their related fractional integrals.

Definition 1. *For a function* $y : [a, b] \to \mathbb{R}^n$, $n - 1 < \varphi \leq n$ *and* $n \in \mathbb{N}$, *the Caputo fractional derivative of order* φ *along with its associated fractional integral are defined as follows [25]:*

$$ {}^{C}_{a}\mathfrak{D}^{\varphi}_{t} y(t) = \frac{1}{\Gamma(n-\varphi)} \int_a^t y^n(s)(t-s)^{n-\varphi-1} ds, \tag{1} $$

$$ {}^{C}_{a}\mathfrak{I}^{\varphi}_{t} y(t) = \frac{1}{\Gamma(\varphi)} \int_a^t y(s)(t-s)^{\varphi-1} ds. \tag{2} $$

Definition 2. *For a function* $y \in H^1(a, b)$ *and* $0 < \varphi < 1$, *the CF fractional derivative of order* φ *and its associated integral [26], are given respectively by:*

$$ {}^{CF}_{a}\mathfrak{D}^{\varphi}_{t} y(t) = \frac{N(\varphi)}{1-\varphi} \int_a^t y'(s) \exp(-\beta(t-s)) ds, \tag{3} $$

$$ {}^{CF}_{a}\mathfrak{I}^{\varphi}_{t} y(t) = \frac{2}{N(\varphi)(2-\varphi)} \left[(1-\varphi) y(t) + \varphi \int_a^t y(s) ds. \right], \tag{4} $$

where, $\beta = \dfrac{\varphi}{1-\varphi}$ *and* $N(\varphi)$ *is the normalization function.*

Definition 3. *For a function* $y \in H^1(a, b)$ *and* $0 < \varphi < 1$, *the ABC derivative of order* φ, *along with its corresponding integral [27], are defined respectively as:*

$$ {}^{ABC}_{a}\mathfrak{D}^{\varphi}_{t} y(t) = \frac{B(\varphi)}{1-\varphi} \int_a^t y'(s) E_{\varphi}(-\beta(t-s)^{\varphi}) ds, \tag{5} $$

$$ {}^{CF}_{a}\mathfrak{I}^{\varphi}_{t} y(t) = \frac{(1-\varphi)}{B(\varphi)} y(t) + \frac{\varphi}{B(\varphi)\Gamma(\varphi)} \int_a^t y(s)(t-s)^{\varphi-1} ds. \tag{6} $$

where, $\beta = \dfrac{\varphi}{1-\varphi}$, E_{φ} *is the ML function and* $B(\varphi)$ *is the normalization function with* $B(0) = B(1) = 1$.

3 Fractional Order Mathematical Model

The current study builds upon the extension of brucellosis model proposed by Al-Hdaibat et al. [24], which captures the interaction dynamics between livestock and humans through both direct contact and environmental exposure. The livestock population is divided into susceptible S(t), infected I(t), and vaccinated V(t) classes, while the level of brucella contamination in the environment is represented by L(t). The human population is categorized into susceptible $S_h(t)$ and infected $I_h(t)$ individuals. The total livestock and human populations at time t are given by $N_1(t) = S(t) + I(t) + V(t)$ and $N_2(t) = S_h + I_h$, respectively. In this model, brucellosis transmission occurs through contact with infected livestock or with pathogens present in the environment. Importantly, humans are assumed not to contribute to onward transmission, neither among themselves nor back to livestock. Susceptible humans may become infected either by direct interaction with infected animals or indirectly through environmental exposure. To explore the impact of different fractional frameworks, we further generalize the model using two alternative non-singular and non-local operators: the CF operator and the ABC operator. Each of these operators brings distinct characteristics in terms of memory kernel and singularity behavior. Thus, the proposed system is formulated under the following frameworks:

Caputo -Fabrizio Sense:

$$ \begin{aligned}
{}^{CF}_{a}\mathfrak{D}^{\varphi}_{t} S(t) &= \Lambda^{\varphi} - \tau_1^{\varphi} \frac{SI}{N_1} - \tau_2^{\varphi} \frac{SL}{N_1} - \nu^{\varphi} S + \omega^{\varphi} V - \kappa_1^{\varphi} S, \\
{}^{CF}_{a}\mathfrak{D}^{\varphi}_{t} L(t) &= \delta^{\varphi} I - \psi^{\varphi} L, \\
{}^{CF}_{a}\mathfrak{D}^{\varphi}_{t} I(t) &= \tau_1^{\varphi} \frac{SI}{N_1} + \tau_2^{\varphi} \frac{SL}{N_1} - \mu^{\varphi} I - \kappa_1^{\varphi} I, \\
{}^{CF}_{a}\mathfrak{D}^{\varphi}_{t} V(t) &= \nu^{\varphi} S - \omega^{\varphi} V - \kappa_1^{\varphi} V, \\
{}^{CF}_{a}\mathfrak{D}^{\varphi}_{t} S_h(t) &= \Lambda_h^{\varphi} - \beta_1^{\varphi} \frac{S_h I}{N_2} - \beta_2^{\varphi} \frac{S_h L}{N_2} - \kappa_2^{\varphi} S_h + r^{\varphi} I_h, \\
{}^{CF}_{a}\mathfrak{D}^{\varphi}_{t} I_h(t) &= \beta_1^{\varphi} \frac{S_h I}{N_2} - \beta_2^{\varphi} \frac{S_h L}{N_2} - \kappa_2^{\varphi} I_h - r^{\varphi} I_h,
\end{aligned} \tag{7} $$

with initial condition:

$$S(0) = S_0, L(0) = L_0, I(0) = I_0, S_h(0) = S_{h,0}, I_h(0) = I_{h,0}.$$

Atangana-Baleaneu Caputo Sense:

$$\begin{aligned}
{}^{ABC}_{a}\mathfrak{D}^{\varphi}_{t} S(t) &= \Lambda^{\varphi} - \tau_1^{\varphi}\frac{SI}{N_1} - \tau_2^{\varphi}\frac{SL}{N_1} - \nu^{\varphi} S + \omega^{\varphi} V - \kappa_1^{\varphi} S,\\
{}^{ABC}_{a}\mathfrak{D}^{\varphi}_{t} L(t) &= \delta^{\varphi} I - \psi^{\varphi} L,\\
{}^{ABC}_{a}\mathfrak{D}^{\varphi}_{t} I(t) &= \tau_1^{\varphi}\frac{SI}{N_1} + \tau_2^{\varphi}\frac{SL}{N_1} - \mu^{\varphi} I - \kappa_1^{\varphi} I,\\
{}^{ABC}_{a}\mathfrak{D}^{\varphi}_{t} V(t) &= \nu^{\varphi} S - \omega^{\varphi} V - \kappa_1^{\varphi} V,\\
{}^{ABC}_{a}\mathfrak{D}^{\varphi}_{t} S_h(t) &= \Lambda_h^{\varphi} - \beta_1^{\varphi}\frac{S_h I}{N_2} - \beta_2^{\varphi}\frac{S_h L}{N_2} - \kappa_2^{\varphi} S_h + r^{\varphi} I_h,\\
{}^{ABC}_{a}\mathfrak{D}^{\varphi}_{t} I_h(t) &= \beta_1^{\varphi}\frac{S_h I}{N_2} - \beta_2^{\varphi}\frac{S_h L}{N_2} - \kappa_2^{\varphi} I_h - r^{\varphi} I_h,
\end{aligned} \tag{8}$$

with initial condition:

$$S(0) = S_0, L(0) = L_0, I(0) = I_0, S_h(0) = S_{h,0}, I_h(0) = I_{h,0}.$$

Table 1: List of model parameters and their biological significance.

Parameters	Description	Sources
Λ	Recruitment rate of susceptible livestock	[24]
τ_1	Transmission rate between healthy and infected livestock	Estimated
τ_2	Transmission rate from environmental pathogens to healthy livestock	Estimated
ν	Vaccination rate of healthy livestock	[24]
ω	Rate at which vaccinated livestock lose immunity	[24]
κ_1	Natural death rate of livestock	[24]
δ	Amount of Brucella bacteria discharged into the environment by livestock	Estimated
ψ	Shedding rate of brucellosis into the environment	Estimated
μ	Culling rate of infected livestock after detection	Estimated
Λ_h	Birth rate of the human population	[24]
β_1	Transmission rate from infected livestock to healthy humans	Estimated
β_2	Transmission rate from environment to healthy humans	Estimated
κ_2	Natural death rate of humans	[24]
r	Recovery rate of infected humans	Estimated

Table 2: Estimated parameter values for the CF and ABC models along with corresponding RMSE values.

Parameters	τ_1	τ_2	μ	δ	ψ	β_1	β_2	r	φ	RMSE
Caputo	0.4353	0.2754	0.0172	0.0108	0.0614	0.3529	0.0367	0.0398	-	9672.4856
CF	0.4405	0.3201	0.04998	0.00102	0.07997	0.2843	0.0367	0.00523	0.91	8382.4671
ABC	0.4872	0.2876	0.01830	0.00100	0.03979	0.3255	0.03562	0.0021	0.98	8305.6242

4 Model analysis

This section is devoted to examining the existence and uniqueness of solutions for the fractional order models (7) and (8), utilizing fixed point theory within the framework of fractional calculus. To simplify the analysis, we proceed under the

assumption that:

$$\begin{aligned}
f_1(S,L,I,V,S_h,I_h) &= \Lambda^{\varphi} - \tau_1^{\varphi}\frac{SI}{N_1} - \tau_2^{\varphi}\frac{SL}{N_1} - \nu^{\varphi}S + \omega^{\varphi}V - \kappa_1^{\varphi}S,\\
f_2(S,L,I,V,S_h,I_h) &= \delta^{\varphi}I - \psi^{\varphi}L,\\
f_3(S,L,I,V,S_h,I_h) &= \tau_1^{\varphi}\frac{SI}{N_1} + \tau_2^{\varphi}\frac{SL}{N_1} - \mu^{\varphi}I - \kappa_1^{\varphi}I,\\
f_4(S,L,I,V,S_h,I_h) &= \nu^{\varphi}S - \omega^{\varphi}V - \kappa_1^{\varphi}V,\\
f_5(S,L,I,V,S_h,I_h) &= \Lambda_h^{\varphi} - \beta_1^{\varphi}\frac{S_hI}{N_2} - \beta_2^{\varphi}\frac{S_hL}{N_2} - \kappa_2^{\varphi}S_h + r^{\varphi}I_h,\\
f_6(S,L,I,V,S_h,I_h) &= \beta_1^{\varphi}\frac{S_hI}{N_2} - \beta_2^{\varphi}\frac{S_hL}{N_2} - \kappa_2^{\varphi}I_h - r^{\varphi}I_h.
\end{aligned} \tag{9}$$

It is further assumed, based on the nature of the physical problem, that the state variables S, L, I, V, S_h, and I_h remain bounded. Consequently, there exist constants M_1, M_2, M_3, M_4, M_5, and M_6 such that:

$$\|S(t)\| < M_1, |L(t)\| < M_2, \|I(t)\| < M_3, \|V(t)\| < M_4, \|S_h(t)\| < M_5, \|I_h(t)\| < M_6.$$

We consider the following vector

$$\begin{aligned}
\chi(t) &= \left[S,L,I,V,S_h,I_h\right],\\
\chi_0 &= \left[S(0),L(0),I(0),V(0),S_h(0),I_h(0)\right],
\end{aligned} \tag{10}$$

and,

$$\mathfrak{S}(t,\chi(t)) = \left[f_1(t,\chi(t)), f_2(t,\chi(t)), f_3(t,\chi(t)), f_4(t,\chi(t)), f_5(t,\chi(t)), f_6(t,\chi(t))\right]', \tag{11}$$

where $\|\chi(t)\| = \max_{1\le i\le 6}|\chi_i(t)|$, $\|\mathfrak{S}\| = \max_{1\le i\le 6}\sum_{j=1}^{3}|\mathfrak{S}_{i,j}(i,\chi(t))|$.

For C-F Model: The C-F fractional integral operator, when applied to system (10), yields

$$\begin{aligned}
S(t) - S(0) &= \frac{2(1-\varphi)}{N(\varphi)(2-\varphi)}\left[f_1(t,S)\right] + \frac{2\varphi}{N(\varphi)(2-\varphi)}\int_0^t f_1(s,S)ds,\\
L(t) - L(0) &= \frac{2(1-\varphi)}{N(\varphi)(2-\varphi)}\left[f_2(t,L)\right] + \frac{2\varphi}{N(\varphi)(2-\varphi)}\int_0^t f_2(s,L)ds,\\
I(t) - I(0) &= \frac{2(1-\varphi)}{N(\varphi)(2-\varphi)}\left[f_3(t,I)\right] + \frac{2\varphi}{N(\varphi)(2-\varphi)}\int_0^t f_3(s,I)ds,\\
V(t) - V(0) &= \frac{2(1-\varphi)}{N(\varphi)(2-\varphi)}\left[f_4(t,V)\right] + \frac{2\varphi}{N(\varphi)(2-\varphi)}\int_0^t f_4(s,V)ds,\\
S_h(t) - S_h(0) &= \frac{2(1-\varphi)}{N(\varphi)(2-\varphi)}\left[f_5(t,S_h)\right] + \frac{2\varphi}{N(\varphi)(2-\varphi)}\int_0^t f_5(s,S_h)ds,\\
I_h(t) - I_h(0) &= \frac{2(1-\varphi)}{N(\varphi)(2-\varphi)}\left[f_6(t,I_h)\right] + \frac{2\varphi}{N(\varphi)(2-\varphi)}\int_0^t f_6(s,I_h)ds.
\end{aligned} \tag{12}$$

Taking into account all the previously stated assumptions, we introduce the following combined vector:

$$\chi(t) = \chi(0) + \frac{2(1-\varphi)}{(2-\varphi)N(\varphi)}\left[\mathfrak{S}(t,\chi)\right] + \frac{2\varphi}{(2-\varphi)N(\varphi)}\int_0^t \mathfrak{S}(s,\chi(s))ds. \tag{13}$$

The following recursive relation is now defined:

$$\chi_n(t) = \chi(0) + \frac{2(1-\varphi)}{(2-\varphi)N(\varphi)}\left[\mathfrak{S}(t,\chi_{n-1})\right] + \frac{2\varphi}{(2-\varphi)N(\varphi)}\int_0^t \mathfrak{S}(s,\chi_{n-1}(s))ds. \tag{14}$$

The difference between subsequent terms in the recursive formula can be expressed as

$$\begin{aligned}
\chi_n(t) - \chi_{n-1}(t) =& \frac{2(1-\varphi)}{(2-\varphi)N(\varphi)}\left[\mathfrak{S}(t,\chi_{n-1}) - \mathfrak{S}(t,\chi_{n-2})\right] + \frac{2\varphi}{(2-\varphi)N(\varphi)}\\
&\times \int_0^t \left[\mathfrak{S}(s,\chi_{n-1}(s)) - \mathfrak{S}(s,\chi_{n-2}(s))\right]ds.
\end{aligned} \tag{15}$$

Let us define $\Psi_n(t) = \chi_n(t) - \chi_{n-1}(t)$, which implies that $\chi_n(t) = \sum_{j=0}^{n} \Psi_j(t)$. By applying the usual supremum norm to both sides of equation (15):

$$\begin{aligned} \|\Psi_n(t)\| &= \|\chi_n(t) - \chi_{n-1}(t)\| \qquad (16)\\ &\leq \frac{2(1-\varphi)}{(2-\varphi)N(\varphi)}\|\mathfrak{S}(t,\chi_{n-1}) - \mathfrak{S}(t,\chi_{n-2})\| + \frac{2\varphi}{(2-\varphi)N(\varphi)} \\ &\quad \times \int_0^t \|\mathfrak{S}(s,\chi_{n-1}(s)) - \mathfrak{S}(s,\chi_{n-2}(s))\|ds. \qquad (17)\end{aligned}$$

Thus, using the Lipschitz constant Υ_1 to propitiate the Lipschitz condition, we get

$$\begin{aligned} \|\chi_n(t) - \chi_{n-1}(t)\| &\leq \frac{2(1-\varphi)}{N(\varphi)(2-\varphi)}\,\Upsilon_1\,\|\chi_{n-1}(t) - \chi_{n-2}(t)\| + \frac{2\varphi}{N(\varphi)(2-\varphi)} \\ &\quad \times \int_0^t \Upsilon_1\|\chi_{n-1}(s) - \chi_{n-2}(s)\|ds, \qquad (18)\\ \|\Psi_n\| &\leq \frac{2(1-\varphi)}{N(\varphi)(2-\varphi)}\,\Upsilon_1\,\|\Psi_{n-1}\| + \frac{2\varphi}{N(\varphi)(2-\varphi)}\int_0^t \Upsilon_1\|\Psi_{n-1}(s)\|ds. \qquad (19)\end{aligned}$$

Theorem 1. *The fractional-order model involving the ABC operator admits a unique solution, provided* $\exists$ *a time* $T > 0$ *and the following condition is satisfied::*

$$\frac{2(1-\varphi)}{N(\varphi)(2-\varphi)}\,\Upsilon_1 + \frac{2\varphi}{N(\varphi)(2-\varphi)}\,\Upsilon_1\,T < 1, \qquad (20)$$

solution exist for the C-F model.

Proof. We have from Eq. (18)

$$\|\Psi_n\| \leq \frac{2(1-\varphi)}{(2-\varphi)N(\varphi)}\,\Upsilon_1\,\|\Psi_{n-1}\| + \frac{2\varphi}{(2-\varphi)N(\varphi)}\int_0^t \Upsilon_1\|\Psi_{n-1}(s)\|ds. \qquad (21)$$

By using the recursive method, we obtain

$$\|\Psi_n\| \leq \|\Psi_n(0)\|\left[\frac{2(1-\varphi)}{N(\varphi)(2-\varphi)}\,\Upsilon_1 + \frac{2\varphi\,\Upsilon_1\,t}{N(\varphi)(2-\varphi)}\right]^n. \qquad (22)$$

To demonstrate that $\chi(t)$ is a solution of system (7), we make the following assumptions

$$\chi(t) - \chi(0) = \chi_n(t) + \mathfrak{A}(t). \qquad (23)$$

Then, we have

$$\begin{aligned} \|\mathfrak{A}(t)\| &= \left\| \begin{aligned} &\frac{2(1-\varphi)}{(2-\varphi)N(\varphi)}\left[F(t,\chi) - F(t,\chi_{n-1})\right] + \frac{2\varphi}{(2-\varphi)N(\varphi)} \\ &\times \int_0^t \Upsilon_1\left[\mathfrak{S}(s,\chi) - \mathfrak{S}(s,\chi_{n-1})\right]ds \end{aligned} \right\|, \qquad (24)\\ &\leq \frac{2(1-\varphi)}{(2-\varphi)N(\varphi)}\,\Upsilon_1\,\|\chi - \chi_{n-1}\| + \frac{2\varphi}{(2-\varphi)N(\varphi)}\,\Upsilon_1\,\|\chi - \chi_{n-1}\|t. \qquad (25)\end{aligned}$$

Repeating this process we get at the point $t = T$,

$$\|\mathfrak{A}(t)\| \leq \left[\frac{2(1-\varphi)}{N(\varphi)(2-\varphi)} + \frac{2\varphi\,\Upsilon_1\,T}{N(\varphi)(2-\varphi)}\right]^{n+1}\Upsilon_1^{n+1}\,M. \qquad (26)$$

As $n \to \infty$, we get $\|\mathfrak{A}(t)\| \to 0$.

Now we prove that the solution of system (7) is unique. For that, we choose $\chi(t)$ and $\chi_1(t)$ are two different solutions then,

$$\|\chi(t)-\chi_1(t)\| = \frac{2(1-\varphi)}{(2-\varphi)N(\varphi)}\|\mathfrak{S}(t,\chi)-\mathfrak{S}(t,\chi_1)\| + \frac{2\varphi}{(2-\varphi)N(\varphi)} \times \int_0^t \|\mathfrak{S}(s,\chi)-\mathfrak{S}(s,\chi_1)\|ds, \tag{27}$$

$$\leq \frac{2(1-\varphi)}{(2-\varphi)N(\varphi)}\,\Upsilon_1\,\|\chi-\chi_1\| + \frac{2\varphi}{(2-\varphi)N(\varphi)}\,\Upsilon_1\,\|\chi-\chi_1\|t. \tag{28}$$

By reducing the equation (28), we get

$$\|\chi(t)-\chi_1(t)\|\left[1-\frac{2(1-\varphi)}{(2-\varphi)N(\varphi)}\,\Upsilon_1-\frac{2\varphi}{(2-\varphi)N(\varphi)}\,\Upsilon_1\,t\right]\leq 0 \tag{29}$$

$$\Longrightarrow \|\chi(t)-\chi_1(t)\|\leq 0, \tag{30}$$

$$\Longrightarrow \chi(t)=\chi_1(t). \tag{31}$$

This confirms that the system governed by the CF derivative yields a unique and existent solution.

For ABC Model:

Now we consider the case involving the ABC derivative. Accordingly, applying the ABC integral operator to equation (10) gives:

$$\chi(t)=\chi(0)+\frac{1-\varphi}{B(\varphi)}\left[\mathfrak{S}(t,\chi)\right]+\frac{\varphi}{\Gamma(\varphi)B(\varphi)}\int_0^t (t-s)^{\varphi-1}\mathfrak{S}(s,\chi(s))ds. \tag{32}$$

By using the recursive formula, we get

$$\chi_n(t)=\chi(0)+\frac{1-\varphi}{B(\varphi)}\left[\mathfrak{S}(t,\chi_{n-1})\right]+\frac{\varphi}{\Gamma(\varphi)B(\varphi)}\int_0^t (t-s)^{\varphi-1}\mathfrak{S}(s,\chi_{n-1}(s))ds. \tag{33}$$

The difference between two consecutive terms is given as:

$$\chi_n(t)-\chi_{n-1}(t)=\frac{1-\varphi}{B(\varphi)}\left[\mathfrak{S}(t,\chi_{n-1})-\mathfrak{S}(t,\chi_{n-2})\right]+\frac{\varphi}{\Gamma(\varphi)B(\varphi)} \times \int_0^t (t-s)^{\varphi-1}\left[\mathfrak{S}(s,\chi_{n-1}(s))-\mathfrak{S}(s,\chi_{n-2}(s))\right]ds. \tag{34}$$

For simplicity, let $\Theta_n(t)=\chi_n(t)-\chi_{n-1}(t)$. Thus,

$$\chi_n(t)=\sum_{j=0}^{n}\Theta_j(t).$$

We evaluate

$$\|\Theta_n(t)\| = \|\chi_n(t)-\chi_{n-1}(t)\| \tag{35}$$

$$= \left\| \frac{1-\varphi}{B(\varphi)}\left[\mathfrak{S}(t,\chi_{n-1})-\mathfrak{S}(t,\chi_{n-2})\right]+\frac{\varphi}{\Gamma(\varphi)B(\varphi)}\int_0^t (t-s)^{\varphi-1} \times \left[\mathfrak{S}(s,\chi_{n-1}(s))-\mathfrak{S}(s,\chi_{n-2}(s))\right]ds \right\|$$

$$\leq \frac{1-\varphi}{B(\varphi)}\|\mathfrak{S}(t,\chi_{n-1})-\mathfrak{S}(t,\chi_{n-2})\| + \frac{\varphi}{\Gamma(\varphi)B(\varphi)}\int_0^t (t-s)^{\varphi-1} \times \|\mathfrak{S}(s,\chi_{n-1}(s))-\mathfrak{S}(s,\chi_{n-2}(s))\|ds. \tag{36}$$

By using Lipshitz condition, we get

$$\|\Theta_n(t)\| \leq \frac{1-\varphi}{B(\varphi)}\,\Upsilon_2\,\|\chi_{n-1}-\chi_{n-2}\| + \frac{\varphi\Upsilon_2}{\Gamma(\varphi)B(\varphi)}\int_0^t (t-s)^{\varphi-1}\|\chi_{n-1}(s)-\chi_{n-2}(s)\|ds, \tag{37}$$

$$\leq \frac{1-\varphi}{B(\varphi)}\,\Upsilon_2\,\|\Theta_{n-1}(t)\| + \frac{\varphi\Upsilon_2}{\Gamma(\varphi)B(\varphi)}\int_0^t (t-s)^{\varphi-1}\|\Theta_{n-1}(s)\|ds. \tag{38}$$

Theorem 2. *The fractional-order model involving the ABC operator admits a unique solution, provided* $\exists$ *a time* $T > 0$ *and the following condition is satisfied:*

$$\frac{(1-\varphi)\Upsilon_2}{B(\varphi)} + \frac{\hat{T}^{\varphi}\Upsilon_2}{B(\varphi)\Gamma(\varphi)} < 1. \tag{39}$$

Proof. We have from equation (38),

$$\|\Theta_n(t)\| \leq \frac{1-\varphi}{B(\varphi)}\,\Upsilon_2\,\|\Theta_{n-1}(t)\| + \frac{\varphi\Upsilon_2}{\Gamma(\varphi)B(\varphi)}\int_0^t (t-s)^{\varphi-1}\|\Theta_{n-1}(s)\|ds. \tag{40}$$

By successive iterations, we have

$$\|\Theta_n(t)\| \leq \left[\frac{(1-\varphi)\Upsilon_2}{B(\varphi)} + \frac{t^{\varphi}\Upsilon_2}{B(\varphi)\Gamma(\varphi)}\right]^n \|\chi_0\|. \tag{41}$$

Hence, (41) is a smooth function and exist, let us suppose that aforementioned function represent the ABC model's solution:

$$\chi(t) - \chi(0) = \chi_n(t) - \mathfrak{Y}_n(t) \tag{42}$$

$$\begin{aligned}\|\mathfrak{Y}_n(t)\| &\leq \frac{1-\varphi}{B(\varphi)}\|\mathfrak{S}(t,\chi) - \mathfrak{S}(t,\chi_{n-1})\| + \frac{\varphi}{\Gamma(\varphi)B(\varphi)}\int_0^t (t-s)^{\varphi-1} \\ &\quad \times \|\mathfrak{S}(s,\chi(s)) - \mathfrak{S}(s,\chi_{n-1}(s))\|ds, \qquad (43)\\ &\leq \frac{1-\varphi}{B(\varphi)}\,\Upsilon_2\,\|\chi - \chi_{n-1}\| + \frac{t^{\varphi}\Upsilon_2}{\Gamma(\varphi)B(\varphi)}\|\chi - \chi_{n-1}\|. \qquad (44)\end{aligned}$$

By successively repeating the process, we get at the point $t = \hat{T}$,

$$\|\mathfrak{Y}_n(t)\| \leq \left[\frac{1-\varphi}{B(\varphi)} + \frac{\hat{T}^{\varphi}}{\Gamma(\varphi)B(\varphi)}\right]^{n+1} \Upsilon_2^{n+1}\,M'. \tag{45}$$

As n approaches infinity, we get $\|\mathfrak{Y}_n(t)\| \to 0$. For clarity on uniqueness of the solution of the ABC model (8), assuming $\bar{\chi}(t)$ be a distinct solution to (10), then

$$\begin{aligned}\|\chi(t) - \bar{\chi}(t)\| \leq &\frac{1-\varphi}{B(\varphi)}\|\mathfrak{S}(t,\chi) - \mathfrak{S}(t,\bar{\chi})\| + \frac{\varphi}{\Gamma(\varphi)B(\varphi)}\int_0^t (t-s)^{\varphi-1} \\ &\times \|\mathfrak{S}(s,\chi(s)) - \mathfrak{S}(s,\bar{\chi}(s))\|ds. \qquad (46)\end{aligned}$$

By utilizing the kernel's Lipshitz condition, we obtain

$$\|\chi(t) - \bar{\chi}(t)\| \leq \frac{1-\varphi}{B(\varphi)}\,\Upsilon_2\,\|\chi - \bar{\chi}\| + \frac{\hat{T}^{\varphi}\Upsilon_2}{\Gamma(\varphi)B(\varphi)}\|\chi - \bar{\chi}\|, \tag{47}$$

which gives

$$\|\chi(t) - \bar{\chi}(t)\|\left(\frac{1-\varphi}{B(\varphi)}\,\Upsilon_2 + \frac{\hat{T}^{\varphi}\Upsilon_2}{\Gamma(\varphi)B(\varphi)}\right) \leq 0, \tag{48}$$

$$\implies \|\chi(t) - \bar{\chi}(t)\| \leq 0. \tag{49}$$

Thus, $\chi(t) = \bar{\chi}(t)$. So, the proof for the uniqueness of the solutions verifies.

5 Parameter estimation and model fitting

In this section, we present the parameter estimation procedure for the proposed fractional-order brucellosis models utilizing the CF and ABC operators. To estimate the model parameters and the associated fractional orders, we employed the lsqcurvefit optimization routine in MATLAB. This routine implements a nonlinear least-squares approach aimed at

minimizing the discrepancy between the simulated outputs and the actual epidemiological data, thereby optimizing the model fit. The parameters estimated through this procedure include the set $\tau_1, \tau_2, \mu, \delta, \psi, \beta_1, \beta_2$, and r governing the transition dynamics between compartments, as well as the fractional-order parameter φ. The fitting process was performed using cumulative human brucellosis cases from mainland China spanning the years 2004 to 2018, as reported in [24]. Table (2) presents the optimized parameter values obtained for both the CF and ABC models. The optimal fractional order was found to be $\varphi = 0.91$ for the CF model and $\varphi = 0.98$ for the ABC model. These values reflect the best agreement between model simulations and real-world epidemiological trends.

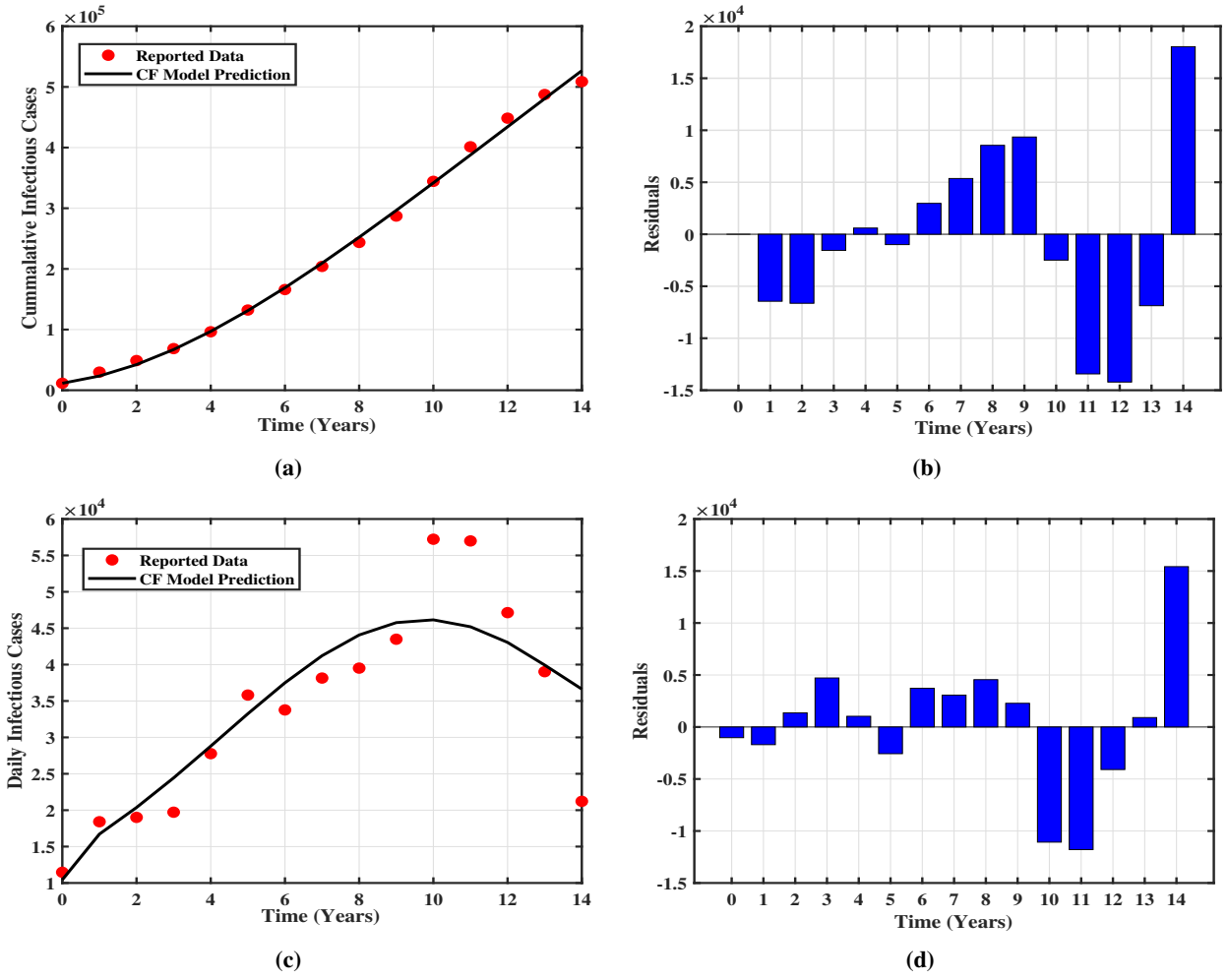

Fig. 1: Time series fitting of real cumulative and daily reported cases by CF fractional-order model along with the corresponding residuals.

Figure (1a) displays the comparison between the model-predicted cumulative brucellosis cases and the actual recorded data for the CF model, while the corresponding residuals are shown in Figure (1b). Additionally, Figure (1c) illustrates the model's performance in capturing daily new infections. A similar graphical representation is provided in Figures (2a)-(2d) for the ABC model. To quantitatively assess the predictive accuracy of the proposed fractional-order models, we computed the root mean square error (RMSE) between the model outputs and the observed data. The estimated parameter values and their corresponding RMSEs are listed in Table (2), alongside the results reported in [24] for the Caputo fractional model. Additionally, for baseline comparison, we evaluated the RMSE for the classical integer-order model, which was found to be 9672.4856. The comparative analysis reveals that all fractional-order formulations (CF, ABC, and Caputo) provide a better fit to the empirical data than the classical model, as evidenced by their lower RMSE values. Among them, the ABC model demonstrates the best performance, yielding the lowest RMSE and thereby signifying superior

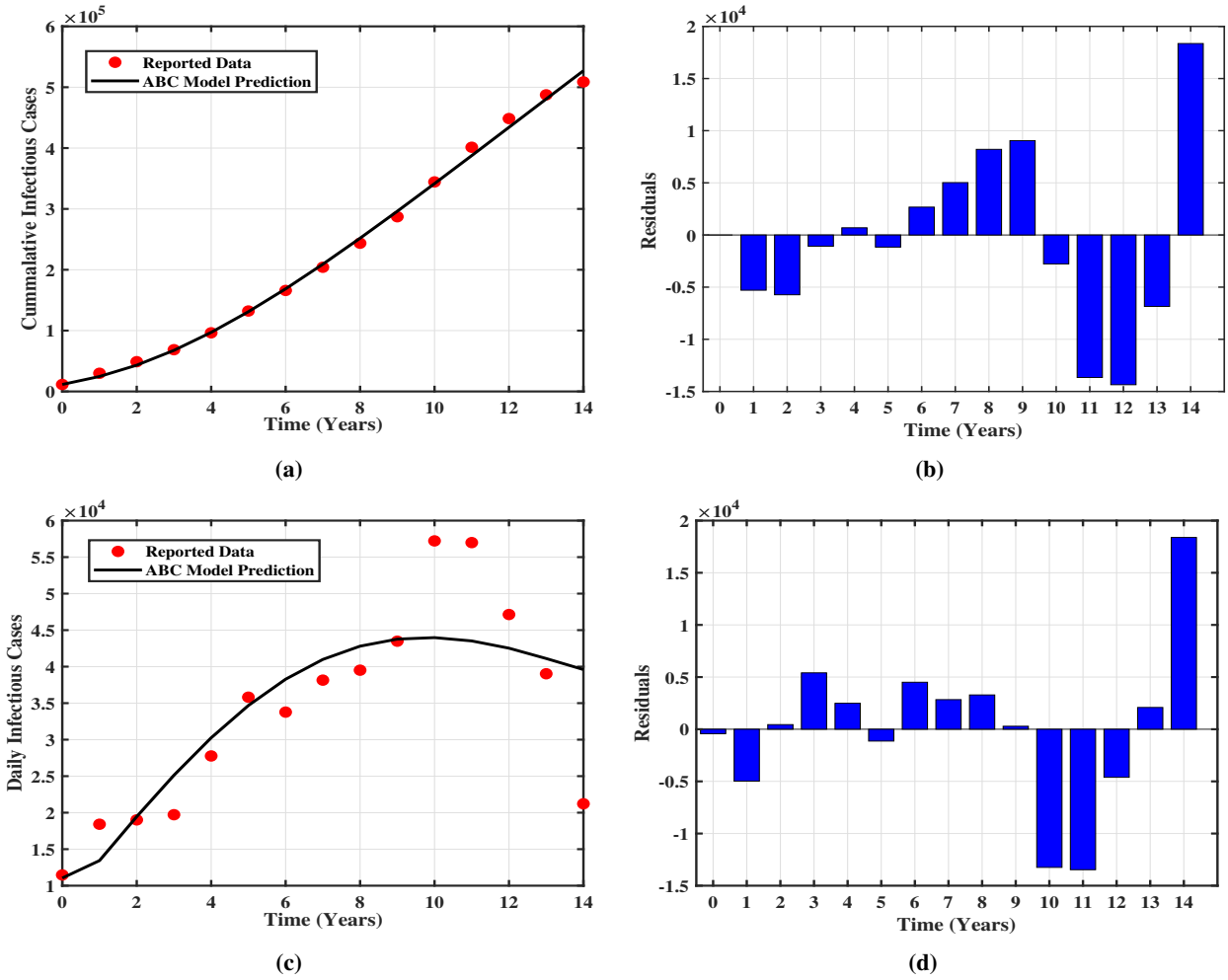

Fig. 2: Time series fitting of real cumulative and daily reported cases by ABC fractional-order model along with the corresponding residuals.

agreement with empirical data. These results highlight the practical relevance of fractional-order modeling in capturing the underlying dynamics of the disease. Despite the increased mathematical complexity, such models offer improved fidelity by incorporating memory and non-local effects—features that are especially pertinent for chronic infectious diseases like brucellosis.

6 Numerical Procedure

In this part, we implement a robust numerical scheme to obtain solutions for the brucellosis disease model, formulated as fractional initial value problems (FIVPs) in (7)–(8), which are reformulated below in a compact form:

$$\begin{aligned} {}_{a}\mathfrak{D}_{t}^{\varphi} y(t) &= \Phi(t, y(t)),\ 0 < t \leq T < \infty, \\ x(0) &= x_0, \end{aligned} \tag{50}$$

where the fractional derivative operator corresponds to either the CF and ABC derivatives, $y(t) = \big(S(t), L(t), I(t), V(t), S_h(t), I_h(t)\big) \in \mathbb{R}_+^6$, and $x_0 = \big(S_0, L_0, I_0, V_0, S_{h,0}, I_{h,0}\big)$. In order to obtin an approximate solution for the problem (50), it is first considered a N-point uniform mesh on $[0, J]$ as $\{ih, i = 0, 1, ..., N\}$.

Also, the time step size is supposed to be $h = \frac{J-0}{N}$ and the numerical approximation of $y(t_i)$ is denoted by y_i, where $t_i = 0 + ih$. In the following, the predictor corrector scheme [28, 29] is used for solving the problem (50).

The corrector and predictor step for CF FIVP is given as:

$$y_{k+1} = x_0 + \frac{\varphi h}{2}\left[\hat{a}_{k+1,k+1}\Phi(t_{k+1}, y^P_{k+1}) + \sum_{j=0}^{k} a_{k+1,j}\Phi(t_j, y_j)\right], \tag{51}$$

$$y^P_{k+1} = x_0 + h\sum_{j=0}^{k} \hat{b}_{k+1,j}\Phi(t_j, y_j), \tag{52}$$

wherein, the weights are described as:

$$\hat{a}_{k+1,k+1} = 1 + \frac{2(1-\varphi)}{\varphi h} \tag{53}$$

$$a_{k+1,j} = \begin{cases} 1; j = 0 \\ 2; 1 \le j \le k \\ 1; j = k+1 \end{cases} \tag{54}$$

$$\hat{b}_{k+1,j} = \begin{cases} 1 + \frac{1-\varphi}{h}; j = k \\ 1; \ , j = 0, ..., k-1. \end{cases} \tag{55}$$

The corrector and predictor step for ABC FIVP is given as:

$$y_{k+1} = x_0 + \frac{h^\varphi}{(\varphi+1)B(\varphi)\Gamma(\varphi)}\left[\hat{a'}_{k+1,k+1}\Phi(t_{k+1}, y^P_{k+1}) + \sum_{j=0}^{k} a'_{k+1,j}\Phi(t_j, y_j)\right], \tag{56}$$

$$y^P_{k+1} = x_0 + \frac{h^\varphi}{B(\varphi)\Gamma(\varphi)}\sum_{j=0}^{k} \hat{b'}_{k+1,j}\Phi(t_j, y_j), \tag{57}$$

wherein, the weights are described as:

$$\hat{a'}_{k+1,k+1} = 1 + \frac{(1-\varphi^2)\Gamma(\varphi)}{h^\varphi}, \tag{58}$$

$$a'_{k+1,j} = \begin{cases} k^{\varphi+1} - (k-\varphi)(k+1)^\varphi; j = 0 \\ (k-j+2)^{\varphi+1} + (k-j)^{\varphi+1} - 2(k-j+1)^{\varphi+1}; 1 \le j \le k \\ 1; j = k+1, \end{cases} \tag{59}$$

$$\hat{b'}_{k+1,j} = \begin{cases} 1 + \frac{(1-\varphi)\Gamma(\varphi)}{h^\varphi}; j = k \\ (k-j+1)^\varphi - (k-j)^\varphi; j = 0, ..., k-1. \end{cases} \tag{60}$$

7 Simulation results and discussion

This section presents the numerical simulation results of the fractional-order brucellosis model formulated under the CF and ABC operators. The predictor-corrector method discussed in Section 6 was employed to obtain numerical solutions for the system. For comparative analysis, simulations were also conducted for the original Caputo formulation as used in the reference model. The simulations were performed using the initial conditions as follows:

$$S_0 = 54,00000, L_0 = 1,00000, I_0 = 10,000, V_0 = 0, S_{h,0} = 1,296,800,000, I_{h,0} = 11472,$$

and optimized parameter values provided in Table (2) and remaining parameter values are obtained as same from [24]. The time evolution of the six compartments is analyzed for fractional orders $\varphi = 1, 0.95, 0.90, 0.85, 0.80$. Figures (3)

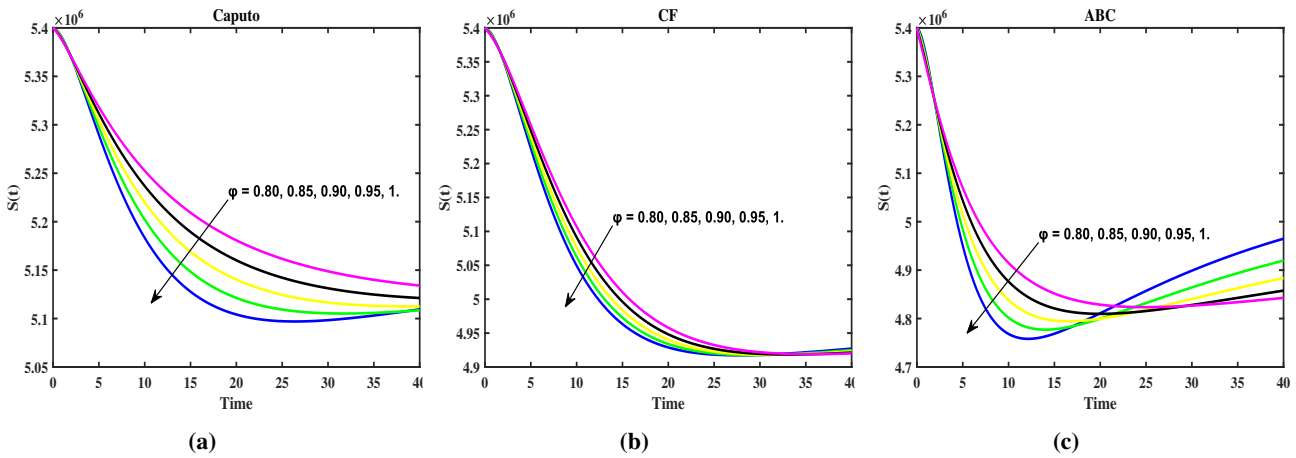

Fig. 3: Time series solution of Susceptible livestock S(t) under (a) Caputo, (b) CF, and (c) ABC operators for different fractional orders.

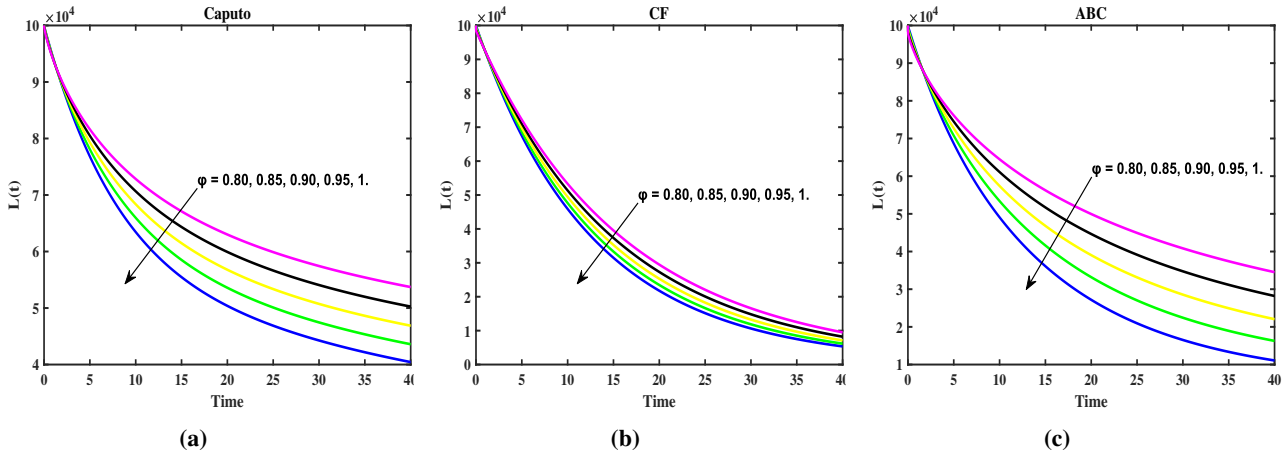

Fig. 4: Time series solution of L(t) under (a) Caputo, (b) CF, and (c) ABC operators for different fractional orders.

through (8) illustrate the behavior of the state variables under each fractional operator. In each Figure, sub-figures (a), (b), and (c) correspond for the Caputo, CF, and ABC derivatives, respectively. In Figures (3), the behavior of the susceptible livestock population S(t) is shown for all three operators. The population consistently declines over time due to new exposures to infection. However, this decline is sensitive to the choice of fractional order. For lower values of φ, the decrease in S(t) is more gradual, signifying that stronger memory effects delay the transition from susceptible to infected states. Comparing across operators, the CF and ABC formulations show lower terminal values of S(t) than the Caputo model, suggesting a slightly faster depletion of the susceptible class under non-singular kernel-based memory. Figures (4) display the decline of brucella concentration in the environment over time. The decay is attributed to the natural degradation of the bacteria and reduced input from infected livestock. Across all operators, lower values of φ correspond to a slower decline in L(t), indicating stronger memory effects. Furthermore, CF and ABC models (Figures (4b) and (4c)) show a more pronounced decay than Caputo (Figure (4a)). Figures (5) illustrate the rise-and-fall trajectory of the infected livestock class I(t), characteristic of infectious outbreaks. For Caputo (Figure (5a)), the infection grows sharply and then stabilizes at a plateau.

In contrast, the CF formulation (Figure 5b) results in a noticeably lower peak followed by a decline, while the ABC model (Figure (5c)) produces the lowest peak and the most significant reduction over time. These results demonstrate that CF and ABC operators suppress infection more effectively, with ABC exhibiting the strongest damping effect on transmission. Furthermore, decreasing the fractional order leads to a delayed and lower peak in all cases, illustrating

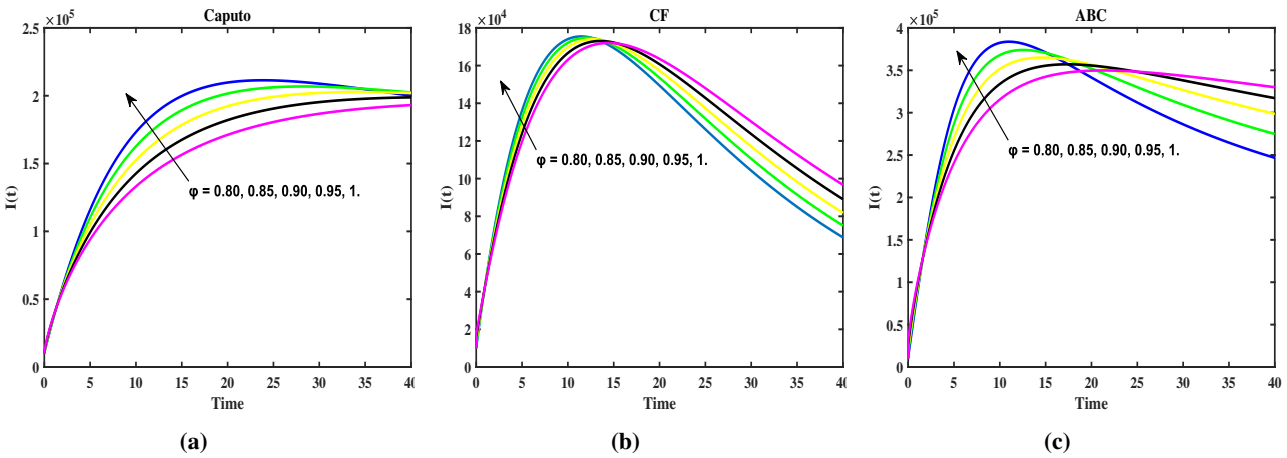

Fig. 5: Time series solution of infected livestock I(t) under (a) Caputo, (b) CF, and (c) ABC operators for different fractional orders.

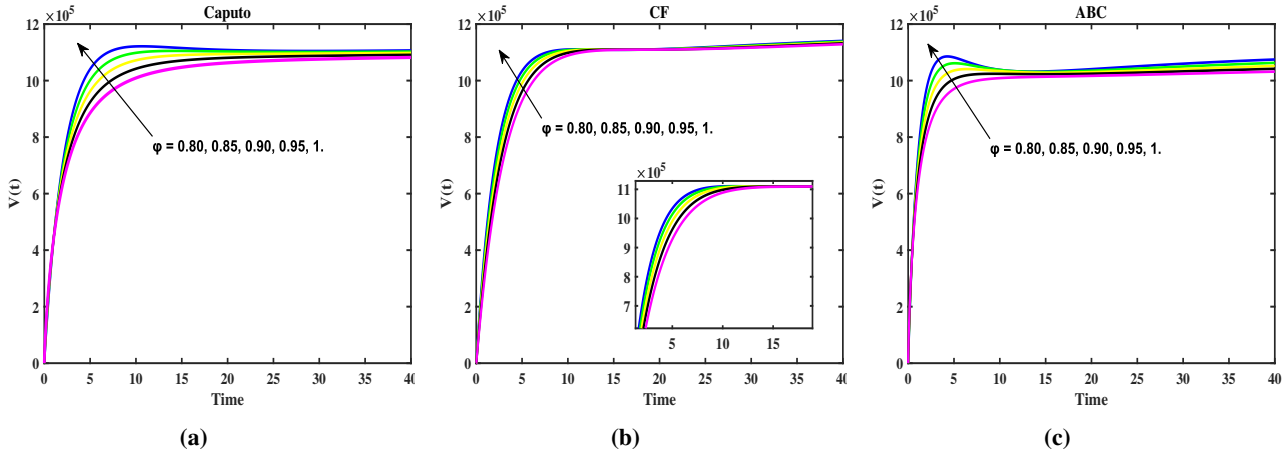

Fig. 6: Time series solution of vaccinated livestock V(t) under (a) Caputo, (b) CF, and (c) ABC operators for different fractional orders.

how memory effects can prolong the infectious period and mitigate the rapid transmission, consistent with the chronic nature of brucellosis. In figures (6), the dynamics of vaccinated livestock V(t) are displayed. Across all formulations, vaccination coverage rises initially and then saturates. The behavior of the susceptible human population $S_h(t)$ is illustrated in Figure (7). In each scenario, the number of susceptible individuals declines over time due to zoonotic transmission from livestock or environmental exposure. Figures (8) show the progression of the infected human population $I_h(t)$. In all cases, the number of infected individuals increases steadily over time. The growth trajectory is noticeably influenced by the fractional order φ larger values of φ lead to a faster and higher accumulation of infections, while lower values result in a more gradual rise. This suggests that as memory effects become stronger (with decreasing φ), the progression of infection slows down. Among the operators, the Caputo formulation yields the most rapid increase, whereas the CF and especially the ABC models exhibit slower accumulation of human infections. Figures (9) further support these findings by displaying the dynamics of compartments L(t), I(t), and $I_h(t)$ under the optimized fractional orders for the CF ($\varphi = 0.91$) and ABC ($\varphi = 0.98$) models in sub-figures (a), (b), and (c), respectively.

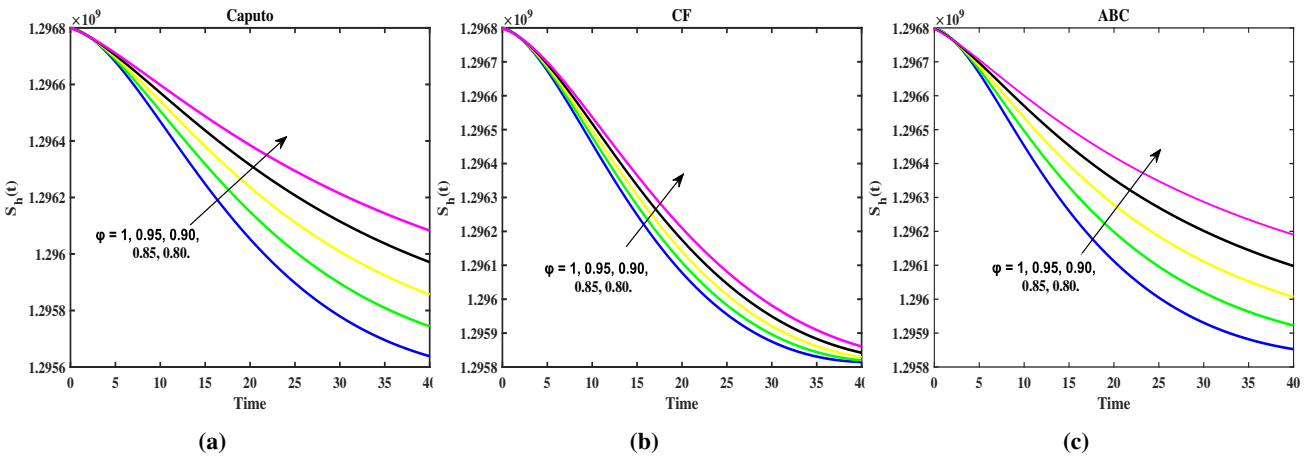

Fig. 7: Time series solution of susceptible human $S_h(t)$ under (a) Caputo, (b) CF, and (c) ABC operators for different fractional orders.

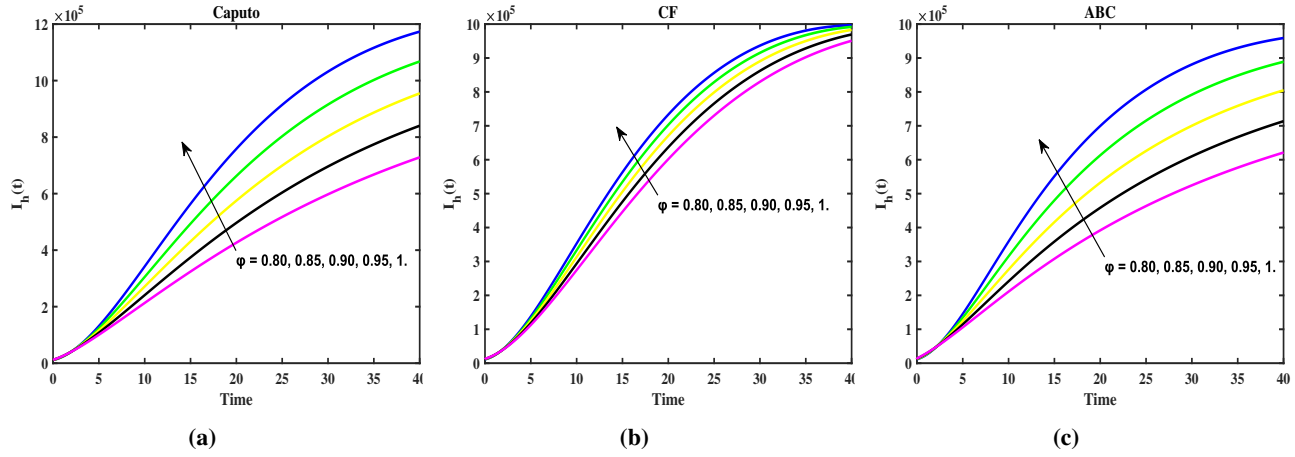

Fig. 8: Time series solution of Infected humans $I_h(t)$ under (a) Caputo, (b) CF, and (c) ABC operators for different fractional orders.

8 Conclusion

In this study, a fractional-order model for the transmission dynamics of brucellosis was developed using the CF and ABC operators. The primary goal was to examine how different fractional operators influence the system's behavior compared to the classical integer-order model and the Caputo formulation. Real epidemiological data from mainland China were employed to estimate model parameters using the least-squares technique, allowing for a quantitative assessment of model performance. A comparative analysis based on the RMSE revealed that all fractional-order models outperformed the classical model in terms of fitting accuracy. Specifically, the ABC operator yielded the lowest RMSE value of 8306, indicating its superior ability to match the observed data. These results highlight the enhanced descriptive power of fractional derivatives, particularly the ABC operator, in capturing the long-term dynamics of chronic infections like brucellosis. Mathematical analysis was also conducted to confirm the existence and uniqueness of solutions for both the CF and ABC models using fixed point theory. To solve the system numerically, we implemented the Adams–Bashforth predictor–corrector method, adapted to handle the nonlocal properties of the fractional operators. Graphical simulations further illustrated the impact of varying the fractional order on each compartment of the model. As the fractional order decreased, a noticeable delay and smoothing in the progression of several compartments was observed, consistent with the memory-dependent nature of the fractional frameworks. The simulations clearly demonstrated that all fractional

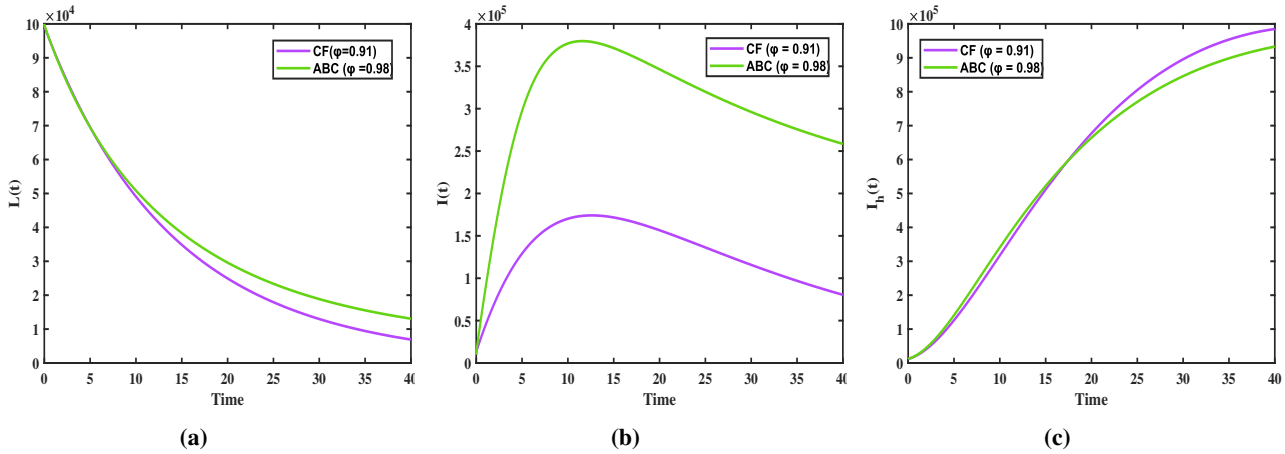

Fig. 9: Simulation of all model compartments under optimized fractional orders: (a) CF model with $\varphi = 0.91$ (b) ABC model with $\varphi = 0.98$.

models provide greater flexibility in capturing the complex temporal behavior of the disease, with the ABC operator showing the most effective response across compartments. This work contributes valuable insight into the applicability of generalized fractional operators in the field of epidemiological modeling and supports their potential use in analyzing other chronic infectious diseases.

Availability of data and materials

The data used in this study is publicly available and has been obtained from the sources cited in the manuscript.

Competing interests

On behalf of all authors, the corresponding author states that there is no conflict of interest.

Authors' contributions

All authors have contributed, read, and approved the manuscript.

Acknowledgments

The author, Sangeeta Kumawat, gratefully acknowledges the financial support provided by the University Grants Commission (UGC), New Delhi, under NTA Reference No. 221610119991.

Ethics approval and consent to participate

Not applicable.

References

[1] K. Zhou, B. Wu, H. Pan, N. Paudyal, J. Jiang, L. Zhang, Y. Li, and M. Yue, ONE health approach to address zoonotic brucellosis: a spatiotemporal associations study between animals and humans, *Frontiers in Veterinary Science* **7** (2020) 521.

[2] M. J. Corbel, Brucellosis in humans and animals, *World Health Organization* (2006).

[3] B. E. Segwagwe, A. Samkange, B. Mushonga, E. Kandiwa, and G. Ndazigaruye, Prevalence and risk factors for brucellosis seropositivity in cattle in Nyagatare District, Eastern Province, Rwanda, *Journal of the South African Veterinary Association* **89**(1) (2018) 1-8.

[4] Y. Wang, C. Xu, S. Zhang, Z. Wang, Y. Zhu, and J. Yuan, Temporal trends analysis of human brucellosis incidence in mainland China from 2004 to 2018, *Scientific Reports* **8**(1) (2018) 15901.

[5] M. Farman, A. Talib, K. S. Nisar, A. Sambas, M. Bayram, and M. Hafez, Investigation of ABPV predict dynamics infection in honeybee colony production: Soft patterns multiscale modeling with fractional approach, *Ain Shams Engineering Journal* **16**(10) (2025) 103626.

[6] S. Mahmoud, M. El-Kady, and M. Abdelhakem, Second kind Chebyshev polynomial differentiation and integration matrices for solving some mathematical models, *Advances in Basic and Applied Sciences* **5**(1) (2025) 1-10.

[7] B. E. Ainseba, C. Benosman, and P. Magal, A model for ovine brucellosis incorporating direct and indirect transmission, *Journal of Biological Dynamics* **4**(1) (2010) 2-11.

[8] W. Beauvais, I. Musallam, and J. Guitian, Vaccination control programs for multiple livestock host species: an age-stratified, seasonal transmission model for brucellosis control in endemic settings, *Parasites & Vectors* **9**(1) (2016) 55.

[9] R. Jan, M. A. Khan, P. Kumam, and P. Thounthong, Modeling the transmission of dengue infection through fractional derivatives, *Chaos, Solitons & Fractals* **127** (2019) 189-216.

[10] S. Kumawat, S. Bhatter, B. Bhatia, S. D. Purohit, H. M. Baskonus, and D. L. Suthar, Novel application of q-HAGTM to analyse Hilfer fractional differential equations in diabetic dynamics, *Mathematics and Computers in Simulation* **238**(C) (2025) 136-149.

[11] W. G. Alharbi, D. M. Almutairi, D. Abdelhamied, M. M. Alzubaidi, M. Areshi, M. El-Kady, and M. Abdelhakem, Pseudospectral fractional differentiation matrices for solving Riccati and Bagley–Torvik fractional models via mixed shifted polynomials, *Fractals* **34**(02) (2026) 2540214.

[12] M. Abdelhakem, Doha M. R, D. Baleanu, M. El-Kady, Shifted ultraspherical pseudo-Galerkin method for approximating the solutions of some types of ordinary fractional problems, *Adv. Differ. Equ.* **2021** (2021) 110.

[13] M. Abdelhakem, Dina Abdelhamied, D. Baleanu, Maryam G. Alshehri, M. El-Kady, Shifted Legendre fractional pseudospectral differentiation matrices for solving fractional differential problems, *Fractals* **30**(1) (2022) 2240038.

[14] D. Baleanu, A. Jajarmi, and M. Hajipour, On the nonlinear dynamical systems within the generalized fractional derivatives with Mittag–Leffler kernel, *Nonlinear Dynamics* **94**(1) (2018) 397-414.

[15] S. Bhatter, S. Kumawat, B. Bhatia, and S. D. Purohit, Analysis of COVID-19 epidemic with intervention impacts by a fractional operator, *An International Journal of Optimization and Control: Theories & Applications (IJOCTA)* **14**(3) (2024) 261-275.

[16] A. S. Biswas, B. H. Aslam, and P. K. Tiwari, Mathematical modeling of a novel fractional-order monkeypox model using the Atangana–Baleanu derivative, *Physics of Fluids* **35**(11) (2023).

[17] S. Kumawat, S. Bhatter, B. Bhatia, S. D. Purohit, and D. L. Suthar, Mathematical modeling of allelopathic stimulatory phytoplankton species using fractal–fractional derivatives, *Scientific Reports* **14**(1) (2024) 20019.

[18] S. Bhatter, S. Kumawat, S. D. Purohit, and D. L. Suthar, Mathematical modeling of tuberculosis using Caputo fractional derivative: a comparative analysis with real data, *Scientific Reports* **15**(1) (2025) 12672.

[19] S. Qureshi and A. Atangana, Mathematical analysis of dengue fever outbreak by novel fractional operators with field data, *Physica A: Statistical Mechanics and its Applications* **526** (2019) 121127.

[20] S. Bhatter, B. Bhatia, S. Kumawat, and S. D. Purohit, Modeling and simulation of COVID-19 disease dynamics via Caputo-Fabrizio fractional derivative, *Computational Methods for Differential Equations* **13**(2) (2025) 494-504.

[21] D. Yapışkan and B. B. İ. Eroğlu, Fractional-order brucellosis transmission model between interspecies with a saturated incidence rate, *Bulletin of Biomathematics* **2**(1) (2024) 114-132.

[22] O. J. Peter, Transmission dynamics of fractional order brucellosis model using caputo–fabrizio operator, *International Journal of Differential Equations* **2020**(1) (2020) 2791380.

[23] G. Alhamzi, A. Chaudhary, S. Sharma, R. Shanker Dubey, and B. S. T. Alkahtani, Characterizing the behavior of solutions in a fractal-fractional model of bovine brucellosis in cattle, *Applied Mathematics in Science and Engineering* **33**(1) (2025) 2458619.

[24] B. Al-Hdaibat, M. A. Khan, I. Ahmad, E. Alzahrani, and A. Akgül, Modeling and analyzing the dynamics of brucellosis disease with vaccination in the fractional derivative under real cases, *Journal of Applied Mathematics and Computing* (2025) 1-22.

[25] S. G. Samko, O. I. Marichev, and A. A. Kilbas, Fractional integrals and derivatives: Theory and applications, *Gordon and Breach Science Publishers* (1993).

[26] M. Caputo and M. Fabrizio, A new definition of fractional derivative without singular kernel, *Progress in Fractional Differentiation & Applications* **1**(2) (2015) 73-85.

[27] A. Atangana and D. Baleanu, New fractional derivatives with nonlocal and non-singular kernel: Theory and application to heat transfer model, *Thermal Science* **20**(2) (2016) 763-769.

[28] K. Diethelm and A. D. Freed, The FracPECE subroutine for the numerical solution of differential equations of fractional order, *Forschung und wissenschaftliches Rechnen* **1999** (1998) 57-71.

[29] C. Li and F. Zeng, The finite difference methods for fractional ordinary differential equations, *Numerical Functional Analysis and Optimization* **34**(2) (2013) 149-179.
[30] Shah Hussain, N. I., Madi, E. N., Bakouri, M., Khan, I., & Koh, W. S. . On the stochastic modeling and forecasting of the SVIR epidemic dynamic model under environmental white noise. *AIMS Mathematics*, **10**(2) (2025) 3983-3999.